International Journal of Heat and Technology
Vol. 43, No. 6, December, 2025, pp. 2090-2104
Journal homepage: http://iieta.org/journals/ijht

A Heat-Transfer-Energy Coupling Model for System-Level Efficiency Optimization in Multi-Node Logistics Networks

Liping Qu

Shijiazhuang College of Applied Technology, Shijiazhuang 050000, China

Corresponding Author Email: 2013010660@sjzpt.edu.cn

https://doi.org/10.18280/ijht.430609

Received: 5 March 2025
Revised: 19 September 2025
Accepted: 20 October 2025
Available online: 31 December 2025

Keywords:
multi-node logistics networks, heat-transfer-energy coupling, entropy production, exergy efficiency, non-equilibrium thermodynamics

ABSTRACT

With the rapid expansion of large-scale, multi-node interconnected logistics networks, a substantial increase in the complexity of coordination among freight dispatching, warehousing and sorting operations, and trunk transportation has led to high energy consumption and declining operational efficiency, elevating operational costs and significantly constraining the low-carbon and sustainable development of the logistics sector. Conventional optimization approaches for logistics networks have primarily relied on operations research paradigms, focusing on localized operational improvements and overlooking the physical mechanisms governing energy transfer, conversion, and dissipation during system operation, which cannot identify the fundamental sources of efficiency loss or theoretically support global energy-efficiency enhancement. In this study, a heat-transfer-energy coupling model for multi-node logistics networks was developed on the basis of non-equilibrium thermodynamics and finite-time thermodynamics. Network node load distributions are mapped onto temperature fields, cargo transportation processes are represented as equivalent heat fluxes, and resource consumption is described as energy conversion processes, systematically quantifying entropy production and exergy destruction induced by irreversible processes within the network and revealing the influence of thermodynamic parameters on system operational efficiency. Furthermore, optimization strategies grounded in thermodynamic criteria were proposed. Numerical case studies demonstrated the effectiveness of the proposed model, explicitly elucidating the quantitative relationships among node temperature uniformity, path thermal conductance characteristics, and system exergy efficiency. Critical sources of exergy destruction within the logistics network were accurately identified. By establishing an explicit heat-transfer-energy coupled model, this work introduces a novel thermodynamic perspective for logistics network efficiency optimization and extends the application of non-equilibrium thermodynamics to non-traditional engineering systems.

1. INTRODUCTION

The integration of global trade and the expansion of e-commerce have driven logistics networks toward large-scale, multi-node interconnected configurations [1, 2], resulting in a pronounced increase in the coordination complexity among inter-node freight dispatching, warehousing and sorting operations, and trunk transportation systems [3-5]. According to available statistics, the global logistics sector accounts for approximately 8-12% of total societal energy consumption, while contributing more than 6% of global carbon emissions. Excessive energy consumption coupled with low operational efficiency has therefore emerged as a critical bottleneck constraining the green and low-carbon transformation of the industry [6]. At the same time, operational costs for logistics enterprises have been substantially elevated, rendering the improvement of network operational efficiency and the reduction of energy consumption urgent challenges [7, 8]. Conventional optimization approaches for logistics networks have primarily been grounded in operations research, graph theory, and systems engineering [9, 10]. These approaches have focused on localized operational improvements, including route planning, inventory control, and node layout optimization, typically through the construction of mathematical programming formulations or heuristic models to identify optimal solutions. Although such methods have been shown to enhance local operational performance under specific scenarios, the physical essence of energy transfer, conversion, and dissipation during system operation has largely remained unaddressed. As a result, intrinsic constraints governing energy flows have been overlooked, fundamental mechanisms responsible for efficiency degradation have not been fully revealed, and robust theoretical support for global energy-efficiency enhancement at the network level has remained limited.

From a thermodynamic perspective, operational phenomena commonly observed in logistics networks—such as transportation delays, node congestion, and empty vehicle movements—are inherently irreversible in nature. These processes exhibit a strong structural analogy to irreversible

thermodynamic phenomena, including heat conduction and energy dissipation [11, 12]. Non-equilibrium thermodynamics and finite-time thermodynamics, which constitute core theoretical frameworks for characterizing energy evolution under irreversible conditions, therefore provide a novel perspective for elucidating the fundamental origins of efficiency losses in logistics networks. By establishing an analogy between logistics processes and thermodynamic processes, abstract operational states of logistics networks can be transformed into quantifiable thermodynamic parameters, thereby offering a physically grounded basis for precise efficiency evaluation and optimization [13]. On the basis of the above considerations, several fundamental scientific questions are raised: How can a thermodynamically consistent heat-transfer-energy coupling model be constructed for multi-node logistics networks to enable a concrete thermodynamic representation of logistics processes? How can the evolution of entropy production and exergy destruction induced by irreversible processes within logistics networks be quantitatively characterized? What intrinsic mechanisms govern the relationships between thermodynamic parameters and system operational efficiency, and how can these mechanisms be exploited to formulate accurate optimization strategies?

In the modeling and optimization of multi-node logistics networks, existing studies have predominantly been conducted within the frameworks of operations research and graph theory. With respect to topological optimization, integer programming and mixed-integer programming models have been extensively employed for node location selection and route planning, with optimization objectives formulated to minimize transportation costs or maximize network coverage [14]. In terms of resource scheduling, heuristic algorithms such as genetic algorithms and particle swarm optimization have frequently been adopted to address multi-objective scheduling problems and to improve resource allocation efficiency. Meanwhile, systems engineering approaches have been applied to construct integrated coordination models at the network level, enabling the joint optimization of warehousing, transportation, and sorting subsystems [15-17]. Despite these advances, existing studies have largely concentrated on operational optimization at the process level, while the physical essence of energy transfer and dissipation has been widely neglected. Energy constraints have seldom been incorporated into modeling frameworks, and quantitative analyses of efficiency degradation induced by irreversible processes have remained scarce. As a result, fundamental improvements in network-level energy efficiency have proven difficult to achieve.

In parallel, thermodynamic theory has progressively extended beyond traditional thermal engineering domains and has demonstrated distinctive value in the analysis and optimization of non-traditional systems. In the field of traffic flow, vehicle density has been analogized to temperature fields, while traffic movement has been represented as heat flux, with traffic evolution models constructed on the basis of Fourier's law to regulate congestion dynamics [18]. In information networks, information transmission has been treated as an energy conversion process, with exergy analysis employed to quantify energy losses. In supply chain systems, thermodynamic cycle concepts have been adopted to model resource flows and to evaluate system stability and efficiency [19, 20]. However, most existing studies have remained at the level of simple analogy. Explicit heat-transfer models and energy conversion models have not been deeply coupled, and, in particular, the intrinsic relationship between temperature-potential-driven energy transfer processes and exergy destruction in logistics networks has not been systematically elucidated. Consequently, precise thermodynamic theoretical support for logistics network efficiency optimization has remained insufficient. Taken together, current research on multi-node logistics network optimization lacks a rigorous representation of the physical nature of energy transfer, while the application of thermodynamic theory in the logistics domain has yet to achieve deep coupling and precise quantification. This gap motivates the present study, whose primary innovations are reflected in the following three aspects:

-First, the limitations of conventional operations research frameworks are transcended through the establishment of a temperature-potential-driven heat-transfer-energy coupling model, enabling a concrete thermodynamic representation of logistics processes.

-Second, entropy production and exergy destruction induced by irreversible processes in logistics networks are quantitatively characterized, and a relational model linking exergy efficiency with network operational parameters is constructed to reveal the thermodynamic origins of efficiency loss.

-Third, logistics network optimization strategies based on the principles of minimum entropy production and maximum exergy efficiency are proposed, providing a novel technical pathway for enhancing global energy efficiency.

The investigation is conducted in response to the aforementioned scientific questions, with the core research components summarized below. A thermodynamic analogy framework for multi-node logistics networks is first established, within which explicit correspondences among node load, cargo transportation, resource consumption, and thermodynamic parameters are defined. Subsequently, a heat-transfer-energy coupling dynamical model is developed to characterize the temporal evolution of node temperature fields and the dynamic behavior of energy transfer along network paths. The coupled model is then numerically solved using the finite-difference method, and its validity is examined through simulation studies based on representative multi-node logistics network cases. The influence mechanisms of key thermodynamic parameters—such as path thermal conductance and node thermal capacitance—on system entropy production and exergy efficiency are further analyzed. Finally, hierarchical optimization strategies encompassing node load balancing, path thermal conductance optimization, and system-level coordinated regulation are formulated on the basis of thermodynamic criteria. To achieve these objectives, the adopted technical route follows a progressive logic of theoretical construction-model solution-simulation verification-mechanism analysis-strategy optimization. Specifically, a thermodynamic analogy framework for logistics networks is constructed on the basis of non-equilibrium thermodynamics, followed by the formulation of a heat-transfer-energy coupled dynamical model. The resulting system of coupled differential equations is numerically solved using the finite-difference method, and a simulation platform is established. Dynamic simulation experiments are then performed using a typical multi-node logistics network as a case study to verify model reliability. Parameter sensitivity analyses are subsequently conducted to elucidate the relationships between thermodynamic

parameters and system operational efficiency. On this basis, targeted optimization strategies are proposed and their effectiveness is systematically evaluated.

The remainder of the study is organized below. First, the fundamental principles of non-equilibrium thermodynamics and finite-time thermodynamics are introduced, and a thermodynamic analogy framework for multi-node logistics networks is constructed, with quantitative mappings established between logistics elements and thermodynamic parameters. Next, coupled equations describing node thermal balance and energy conversion, as well as path heat transfer and exergy destruction, are formulated to develop an integrated thermodynamic efficiency model of the network, together with explicit model assumptions and boundary conditions. Subsequently, a representative multi-node logistics network case is designed, baseline parameters are specified, and numerical solutions are obtained using the finite-difference method, with simulation results employed to validate model effectiveness. Thereafter, sensitivity analyses of key parameters are carried out to reveal the evolution mechanisms of entropy production and exergy destruction, as well as the intrinsic relationships between exergy efficiency and network operational states. Based on the principles of minimum entropy production and maximum exergy efficiency, hierarchical optimization strategies at the node, path, and system levels are then proposed and validated. Finally, the main conclusions are summarized, the core innovations are distilled, research limitations are discussed, and directions for future research are outlined. Through this structured progression, a comprehensive research framework encompassing theory, modeling, validation, analysis, and optimization is established.

2. THEORETICAL FOUNDATIONS AND THERMODYNAMIC ANALOGY SYSTEM

2.1 Core thermodynamic theoretical basis

Non-equilibrium thermodynamics constitutes a fundamental theory for characterizing the evolution of energy in irreversible processes. Its core theoretical underpinning is provided by the entropy production principle articulated by Prigogine, which states that the entropy production rate of a system undergoing any irreversible process is always non-negative, expressed as $\dot{S}_{gen} \geq 0$, where $\dot{S}_{gen}$ denotes the entropy generated per unit time within the system. This principle explicitly identifies irreversibility as the fundamental source of entropy production, while the accumulation of entropy production directly reflects the degree of degradation in energy utilization efficiency. In non-equilibrium systems, the entropy production rate is intrinsically related to thermodynamic forces and thermodynamic fluxes. Within the linear regime, this relationship is governed by the Onsager reciprocal relations, according to which thermodynamic fluxes are linearly proportional to the corresponding thermodynamic forces. Outside the linear regime, nonlinear constitutive relations are required to describe this coupling. This relationship provides a rigorous theoretical basis for quantifying energy losses induced by irreversible phenomena such as delays and congestion in logistics networks. Meanwhile, finite-time thermodynamics addresses the limitations of classical thermodynamics by explicitly incorporating time constraints into the analysis of energy conversion processes, with a particular focus on efficiency limits under finite-time operation. Its central analytical tool is exergy analysis. Exergy, as a key measure of energy quality, is defined as the maximum useful work that a system can deliver under specified environmental conditions. The exergy efficiency of a logistics network can be expressed as $\eta_{ex}=E_{ex,out}/E_{ex,in}$, where $E_{ex,out}$ represents the effective output exergy of the system and $E_{ex,in}$ denotes the total input exergy. Exergy destruction is quantified by the difference between total input exergy and effective output exergy, given by $I=E_{ex,in}-E_{ex,out}$. This quantity fundamentally characterizes the degradation of energy quality caused by irreversible processes. As such, exergy destruction serves as a precise thermodynamic metric for constructing an efficiency evaluation framework for logistics networks.

2.2 Thermodynamic analogy definition for multi-node logistics networks

The construction of a thermodynamic analogy system for multi-node logistics networks is initiated at the node level, where precise correspondences between key logistics elements and thermodynamic parameters are established to provide a foundation for subsequent coupled model formulation. Node temperature is introduced to characterize node processing intensity and resource tightness. Its quantification is defined by the relative relationship between node load and processing capacity, expressed as $T_i = k\cdot(Q_i/P_i)$, where T_i denotes the temperature of node i, k is a scaling coefficient, Q_i represents the volume of goods awaiting processing at the node, and P_i denotes the corresponding processing capacity. A higher node temperature indicates a more saturated operational state and a greater degree of congestion, whereas a lower temperature reflects a relatively idle state with surplus processing capacity. Node thermal capacitance is employed to represent the buffering and load-absorption capability of a node. This parameter is defined as a composite quantitative measure reflecting factors such as storage capacity and redundancy in processing equipment. A larger thermal capacitance implies a reduced sensitivity of node temperature to load fluctuations, thereby indicating a stronger capability to absorb load shocks. The internal heat source of a node is used to characterize the rate at which internal load is generated within a unit time interval. Its magnitude is equivalent to the order arrival rate or cargo throughput per unit time. A positive internal heat source corresponds to an inflow of load into the node, which directly drives an increase in node temperature. The effective work output of a node represents the useful resource output associated with cargo processing activities. It is quantified as the value of goods processed through operations such as sorting and storage per unit time. To ensure consistency with thermodynamic energy parameters, this output is converted into a unified energy-equivalent unit.

At the path level, the thermodynamic analogy focuses on inter-node cargo transfer processes, with the core objective of establishing an equivalent relationship between material flow and heat transfer. Path thermal conductance is introduced to characterize the smoothness of cargo transfer between nodes and is defined as a composite quantitative measure integrating transportation capacity, transport frequency, and operational efficiency along the path. A larger thermal conductance corresponds to a lower thermal resistance, indicating reduced resistance to cargo transfer and higher flow efficiency along the path. Path heat flux is employed to represent the intensity

of cargo transfer between nodes. This transfer process is driven by the temperature potential difference between nodes. By analogy with Fourier's law, the quantitative relationship is expressed as $\dot{P}_{ij} = G_{ij} \cdot (T_i - T_j)$, where $\dot{P}_{ij}$ denotes the path heat flux between nodes i and j, G_{ij} represents the path thermal conductance, and T_i and T_j are the temperatures of the respective nodes. This formulation explicitly establishes a linear relationship between temperature potential difference and cargo transfer intensity. Path exergy destruction is introduced to characterize irreversible energy losses occurring during cargo transportation. Its primary quantitative expression is given by $Ex_{d,ij} = \dot{P}_{ij} \cdot (1 - T_{env}/T_{avg})$, where T_{env} denotes the environmental temperature, corresponding to the ideal operating state of the logistics network and T_{avg} represents the average temperature along the path. In addition, frictional losses arising during transportation are considered, for which exergy destruction may alternatively be quantified as proportional to the square of the transport flow velocity. These two formulations respectively capture the intrinsic nature of path-level irreversibility from the perspectives of temperature potential differences and mechanical energy loss.

At the system level, core thermodynamic indicators are introduced to provide an integrated evaluation of the overall operational state and efficiency of multi-node logistics networks. These indicators represent an aggregation and elevation of thermodynamic parameters defined at both node and path levels. Total entropy production is employed to characterize the overall degree of irreversibility within the system and is defined as the sum of entropy production contributions from all nodes and all paths, expressed as $S_{gen} = \sum S_{gen,i} + \sum S_{gen,ij}$, where $S_{gen,i}$ denotes the entropy production at node i and $S_{gen,ij}$ represents the entropy production along path ij. The accumulated total entropy production directly reflects the combined effects of irreversible phenomena such as delays, congestion, and empty vehicle movements within the logistics network and serves as a core thermodynamic metric for assessing system-level energy dissipation. Exergy efficiency is employed to characterize the energy utilization efficiency of the system and is defined as the ratio of total effective output exergy to total input exergy, given by $\eta_{ex} = E_{ex,out}/E_{ex,in}$. The total input exergy encompasses the energy-equivalent contributions of all resources investment during system operation, including fuel, electricity, and labor, while the total output exergy corresponds to the value flow embodied in goods delivered on time and without loss. Exergy efficiency thus provides a direct quantitative measure of the capability of the logistics network to convert input resources into effective value and constitutes a core indicator for evaluating overall system operational efficiency.

3. CONSTRUCTION OF THE HEAT-TRANSFER-ENERGY COUPLING MODEL FOR MULTI-NODE LOGISTICS NETWORKS

3.1 Model assumptions and boundary conditions

The rational formulation of model assumptions and boundary conditions constitutes a prerequisite for ensuring both the physical validity and the computational tractability of the heat-transfer-energy coupling model. These assumptions are established in accordance with the operational characteristics of logistics networks and standard thermodynamic modeling principles, with a balance maintained between model fidelity and computational complexity. First, node temperature evolution is assumed to be continuous and differentiable with respect to time. This assumption is motivated by the gradual nature of load variations in logistics networks, as processes such as order arrivals and cargo sorting occur in continuous time. Consequently, fluctuations in node processing intensity do not exhibit abrupt discontinuities. As temperature is employed as a surrogate measure of load intensity, its temporal evolution is therefore assumed to satisfy continuity and differentiability conditions, thereby providing a mathematical foundation for the formulation of dynamic differential equations. Second, path heat flux is assumed to be driven by temperature potential differences. This assumption is grounded in the fundamental thermodynamic principle that energy transfer is governed by potential gradients and is further supported by the practical observation that cargo naturally flows from highly loaded nodes toward less loaded nodes within logistics networks. The adoption of this assumption ensures the physical rationality of the heat flux model. Finally, the effects of extreme external disturbances on instantaneous network dynamics are neglected. Events such as severe natural disasters and sudden public emergencies are characterized by low probability and high destructiveness and are considered beyond the scope of routine logistics network operation. By excluding such disturbances, analytical focus is placed on the intrinsic operational mechanisms of the network. The incorporation of extreme scenarios may be addressed through subsequent model extensions if required.

The specification of boundary conditions serves to define the applicability range and initial state of the model and primarily includes initial conditions and boundary constraints. Initial conditions are defined by the initial temperature and initial load of each node at the reference time. Initial node temperatures are calibrated using historical operational data, with corresponding temperature levels determined from statistically averaged historical load intensities. Initial loads are specified using the actual volume of goods awaiting processing at each node at the modeling time, thereby ensuring consistency between the model's initial state and real network conditions. Boundary constraints consist of three primary components. The first is the upper limit of node processing capacity, reflected as a maximum allowable node temperature. When this threshold is reached, the node is considered to be operating at full capacity, and any additional load input is assumed to induce congestion. This upper bound is determined by physical constraints such as storage capacity and the rated throughput of sorting equipment. The second constraint is the upper limit of path transportation capacity, corresponding to the maximum allowable path thermal conductance. This limit is governed by factors such as the rated load capacity of transportation vehicles and the upper bound of transportation frequency, thereby ensuring that modeled heat flux does not exceed actual path carrying capabilities. The third constraint assumes a constant environmental temperature. The environmental temperature represents an ideal operating reference state of the logistics network, corresponding to an optimal load distribution with no congestion or delay. Its value is determined based on industry best-practice performance benchmarks and is maintained constant throughout model execution, providing a reference for the calculation of exergy destruction.

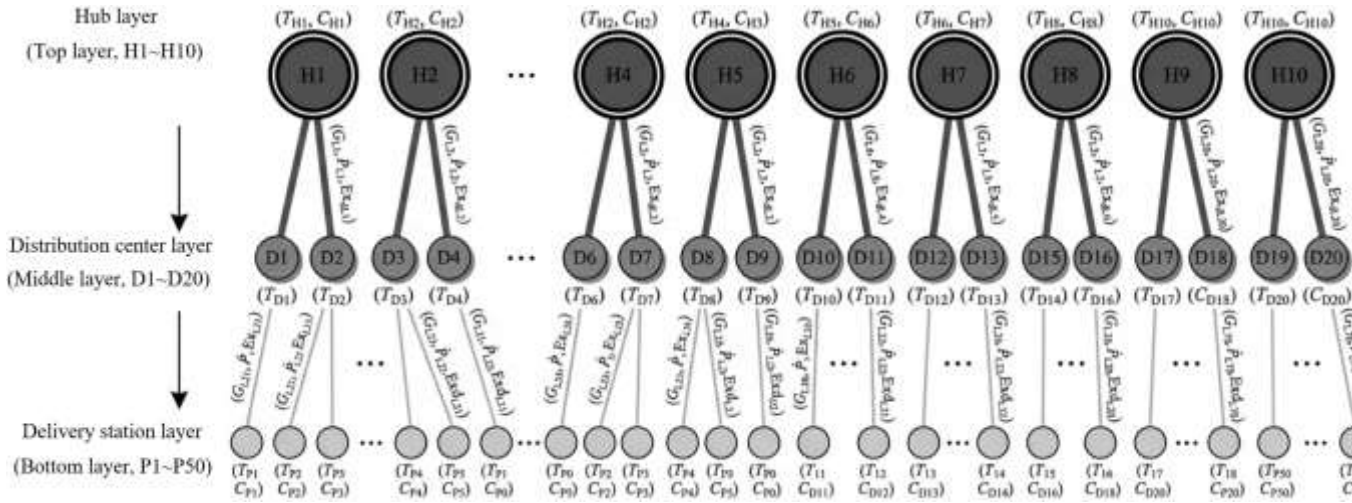

Figure 1. Schematic diagram of a three-tier multi-node logistics network topology

Figure 1 illustrates a large-scale three-tier multi-node logistics network topology, which is composed of 10 hub nodes at the top layer (H1-H10), 20 distribution center nodes at the middle layer (D1-D20), and 50 delivery station nodes at the bottom layer (P1-P50). A hierarchical transshipment logic of "hub-distribution center-delivery station" is adopted. The connectivity rules are defined below. Each hub node in the top layer is connected to two distribution center nodes in the middle layer. Each distribution center node further radiates connections to delivery station nodes in the bottom layer, with the first ten distribution centers each connected to three delivery stations and the remaining ten connected to two delivery stations. This configuration ensures an exact correspondence between the hierarchical structure and the total number of nodes across the three tiers.

3.2 Coupled node thermal balance-energy conversion equation

On the basis of the first law of thermodynamics and the node-level thermodynamic analogy defined above, a coupled node thermal balance-energy conversion equation is formulated to characterize the dynamic evolution of node temperature and the associated energy conversion processes. As a fundamental energy conversion unit within a logistics network, a node satisfies the principle that the rate of change of its thermodynamic energy is equal to the difference between energy input and energy output. In the context of a logistics network, this principle is expressed by equating the product of node thermal capacitance and the time derivative of node temperature to the net heat flux, the internal heat source input, and the effective work output. The governing equation is given by:

$$C_i \cdot \frac{dT_i}{dt} = \sum_j [\, G_{ij} \cdot (T_j - T_i)] + Q_{int,i} - W_{out,i} \tag{1}$$

where, the left-hand side represents the rate of change of thermodynamic energy at node i; C_i denotes the node thermal capacitance, characterizing the capacity of the node to store energy; and dT_i/dt is the temporal rate of change of node temperature, which directly reflects the dynamic variation of node load intensity.

The terms on the right-hand side correspond to the energy input and output processes associated with node operation. The term $\sum_j [\, G_{ij} \cdot (T_j - T_i)]$ represents the net heat flux transmitted to node i from neighboring nodes through connecting paths, where G_{ij} denotes the path thermal conductance between nodes i and j and $(T_j - T_i)$ is the temperature potential difference between the two nodes. When $T_j > T_i$, this term is positive, indicating that cargo flows from node j to node i, thereby contributing an energy input to node i. The term $Q_{int,i}$ denotes the internal heat source of the node, which characterizes the energy input associated with internal load generation. Its magnitude is equivalent to the order arrival rate per unit time and thus constitutes an energy input term. The term $W_{out,i}$ represents the effective work output of the node, corresponding to the useful energy converted during cargo processing operations. Its value is quantified as the value of goods processed per unit time and is treated as an energy output term. Through this coupled equation, a deep integration between logistics processes and thermodynamic processes is achieved. Node-level cargo handling and inter-node cargo transfer are translated into quantifiable energy conversion and thermal balance processes. By solving this equation, the temporal distribution of node temperatures across the network can be obtained, thereby providing a basis for subsequent analysis of network operational states and efficiency degradation. All parameters in the equation are expressed using unified energy units to ensure dimensional consistency. Parameters that are not inherently expressed in energy units are converted through appropriate energy equivalence coefficients, which are determined based on the average energy consumption associated with unit cargo transportation and sorting operations.

3.3 Coupled path heat transfer-exergy destruction equation

As the primary carrier of cargo transfer in multi-node logistics networks, each path requires a coupled heat-transfer-exergy destruction formulation that integrates Fourier's law of heat conduction with exergy analysis theory, thereby enabling a deep coupling between cargo flow processes and thermodynamic heat transfer and energy dissipation mechanisms. On the basis of Fourier's law, the intensity of path heat flux is jointly determined by the temperature potential difference between nodes and the path thermal conductance. The governing heat transfer equation is

expressed as:

$$\dot{P}_{ij}=G_{ij}\cdot(T_i-T_j) \tag{2}$$

where, $\dot{P}_{ij}$ denotes the path heat flux between nodes i and j, representing the cargo transfer rate per unit time; G_{ij} is the path thermal conductance, which is quantified as an integrated measure of transportation capacity, operational efficiency, and transport frequency. The relative importance of these indicators is determined using the analytic hierarchy process, allowing for the normalized integration of multi-dimensional parameters. The term $T_i - T_j$ represents the temperature potential difference between the two nodes and determines the direction of heat flux. When $T_i > T_j$, heat flux is transferred from node i to node j, corresponding to the natural flow of cargo from a highly loaded node toward a less loaded node. This formulation strictly adheres to the fundamental thermodynamic principle that energy transfer is driven by potential gradients. All parameters are converted into unified energy-based dimensions through appropriate energy equivalence coefficients, thereby ensuring both the physical validity and mathematical rigor of the proposed model.

Building upon the heat transfer formulation, a coupled path-level exergy destruction equation is constructed in conjunction with exergy analysis theory to quantify irreversible energy losses during cargo transportation processes. The governing equation is expressed as:

$$Ex_{d,ij}=\dot{P}_{ij}\cdot\left(1-\frac{T_{env}}{T_{avg}}\right)+\alpha\cdot P_{ij}^2 \tag{3}$$

where, the first term represents exergy destruction induced by temperature potential differences, reflecting the degradation of energy quality during cargo transfer under non-ideal temperature distributions. Here, T_{env} denotes the constant environmental temperature, corresponding to the ideal operating state of the logistics network, while T_{avg} denotes the average temperature along the path, calculated as the arithmetic mean of the temperatures at nodes i and j. The second term represents dissipative exergy destruction. By analogy with frictional heat generation in fluid flow, this term characterizes irreversible energy consumption arising from phenomena such as empty vehicle movements, road congestion, and loading-unloading losses during transportation. The coefficient α is a dissipation parameter, whose value is calibrated using operational data from real logistics networks through linear regression methods. Through this formulation, a deep coupling between heat transfer and exergy destruction is achieved. While path heat flux is governed by node temperature potential differences, exergy destruction is jointly influenced by both temperature potential differences and heat flux intensity. An increase in heat flux not only directly amplifies temperature-driven exergy destruction but also significantly magnifies dissipative exergy destruction through the quadratic dependence. As a result, the intrinsic mechanisms of irreversible energy loss along logistics network paths are accurately captured.

3.4 System-level thermodynamic efficiency model

The construction of a system-level thermodynamic efficiency model requires the integration of the coupled equations at both node and path levels. On the basis of fundamental thermodynamic principles, two core performance indicators—total entropy production and exergy efficiency—are established to comprehensively evaluate the operational efficiency of multi-node logistics networks from the perspectives of irreversible loss magnitude and energy utilization quality. The total entropy production model is formulated based on the additivity principle of entropy production, which states that the total entropy production of a system is equal to the algebraic sum of entropy production contributions from all constituent components. Accordingly, the total entropy production of a multi-node logistics network is expressed as the sum of entropy production at all nodes and along all paths, given by:

$$S_{gen}(t)=\sum_i S_{gen,i}(t)+\sum_{ij} S_{gen,ij}(t) \tag{4}$$

where, $S_{gen,i}(t)$ denotes the entropy production at node i at time t, which arises jointly from irreversible processes associated with internal heat source input, effective work output, and heat transfer. The term $S_{gen,ij}(t)$ represents the entropy production along path ij at time t, which exhibits a quantitative relationship with path exergy destruction and can be evaluated as the ratio of exergy destruction to the corresponding temperature level.

Owing to its explicit time dependence, the evolution of $S_{gen}(t)$ directly reflects the accumulation of irreversible losses within the system and provides a fundamental basis for analyzing temporal variations in system operating states.

On the basis of the total entropy production model, a system-level exergy efficiency model is further constructed to quantify the quality of energy utilization. The governing expression is given by:

$$\eta_{ex}(t)=\frac{\sum_i W_{out,i}(t)}{\sum_i W_{in,i}(t)+\sum_{ij} E x_{d,ij}(t)} \tag{5}$$

where, the numerator represents the total effective output exergy of the system at time t, obtained as the sum of effective work outputs from all nodes and reflecting the useful value generated during system operation. The denominator corresponds to the total input exergy at time t, which consists of two components. The first component is the input resource energy $W_{in,i}(t)$ at each node, encompassing all resources investment during node operation, including fuel, electricity, and labor, which are converted into standardized energy units through unified energy equivalence coefficients. The second component is the path-level exergy destruction $Ex_{d,ij}(t)$, representing irreversible energy losses incurred during transportation processes. As these losses originate from the degradation of the quality of input energy, they must be included in the calculation of total input exergy. Through this formulation, parameters at node and path levels are systematically integrated within a unified framework. The exergy efficiency $\eta_{ex}(t)$ takes values within the interval (0,1], where values closer to unity indicate higher energy utilization quality and superior operational efficiency. Together, the total entropy production and exergy efficiency models characterize system performance from two complementary dimensions: total entropy production reflects the absolute magnitude of irreversible losses, while exergy efficiency captures the relative quality of energy utilization. These indicators mutually reinforce one another and provide a comprehensive

and precise thermodynamic basis for subsequent model analysis and optimization strategy development. Figure 2 shows the architecture of the system-level thermodynamic efficiency model.

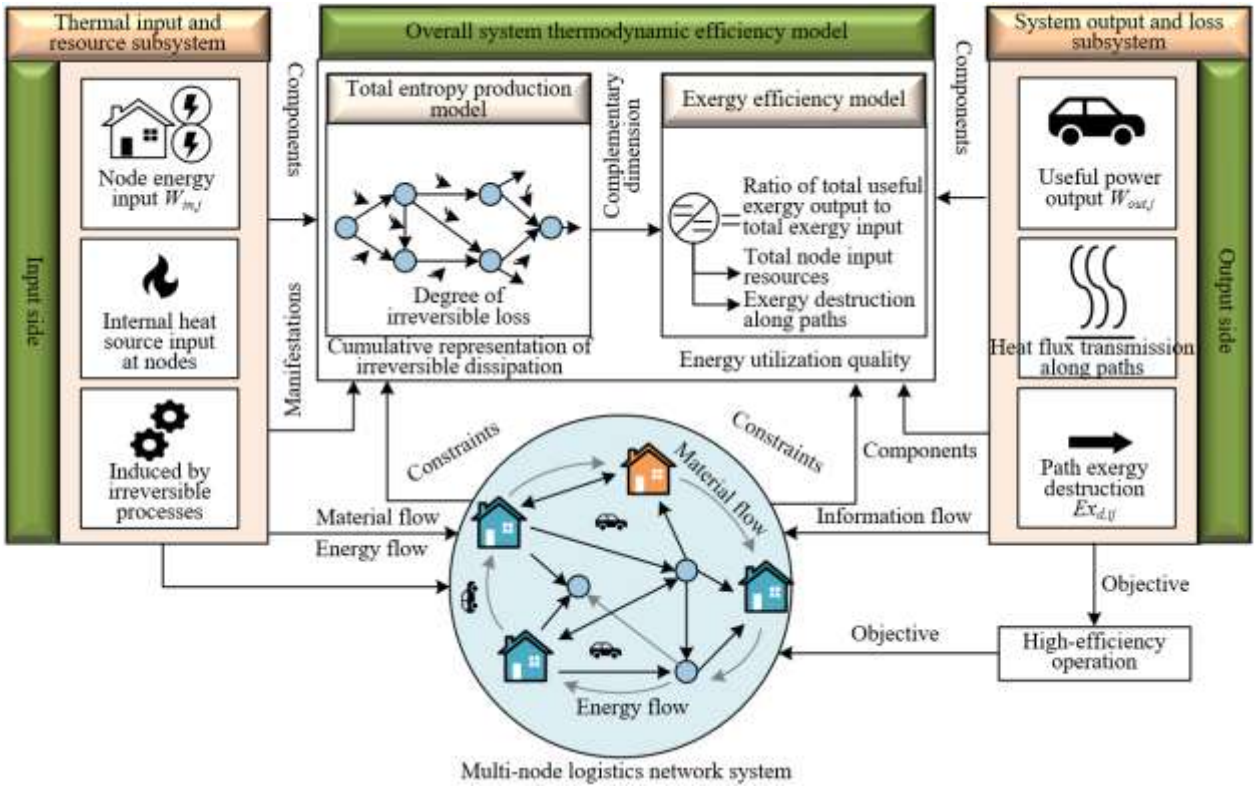

Figure 2. Architecture of the system-level thermodynamic efficiency model

4. MODEL SOLUTION AND CASE SIMULATION VALIDATION

4.1 Case configuration and parameter calibration

To validate the effectiveness and practical applicability of the proposed heat-transfer-energy coupling model, a representative three-tier multi-node logistics network topology is designed for case-based simulation. The network consists of 10 hub nodes, 20 distribution centers, and 50 delivery stations, forming a hierarchical "hub-distribution center-delivery station" structure. Within this topology, each hub node is directly connected to multiple distribution centers, and each distribution center is connected to two delivery stations. The baseline parameters for the case simulation are specified across two dimensions: node-level parameters and path-level parameters. Node-level parameters include thermal capacitance, initial temperature, and dynamically varying order loads, while path-level parameters include path thermal conductance and dissipation coefficients. To ensure model realism and reliability, all baseline parameters are derived from actual operational data obtained from a large regional express logistics enterprise. Dynamic order loads are extracted through time-series analysis of historical order data for the selected region. Parameters such as node thermal capacitance, initial temperature, and path thermal conductance are initially estimated based on the enterprise's warehouse equipment configuration, node processing capacities, and transportation route characteristics. These parameters are subsequently calibrated using the least-squares method, such that the deviation between the simulated baseline operational states and the corresponding real-world operational data is constrained within 5%, ensuring that the model is capable of accurately capturing the operational characteristics of real-world logistics networks.

4.2 Simulation results and model validity verification

The simulation results are presented through a combination of quantitative tabular data and visualized graphical analysis. Model validity is examined from three primary perspectives: the evolution of node temperature fields, the distribution of path heat flux and exergy destruction, and the overall effectiveness of the proposed model. All reported data are obtained from a continuous 8-hour dynamic simulation of the case network, with a temporal resolution of 1 hour. The dynamic evolution of the node temperature field is characterized by the quantified temperature values of all nodes at successive time steps.

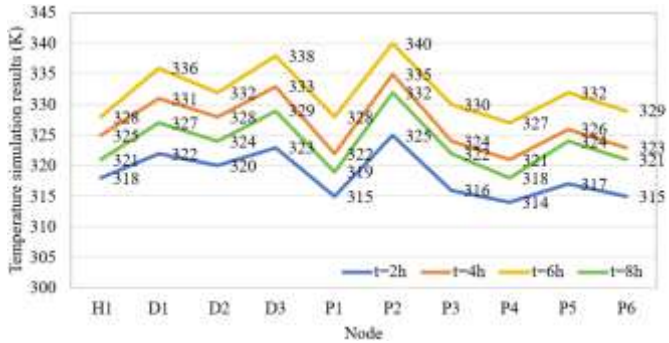

Figure 3. Simulated node temperature distribution at representative time points

Figure 3 illustrates the simulated node temperature distribution at representative time points, covering all nodes across the hub, distribution center, and delivery station layers. The spatiotemporal evolution patterns of temperatures are thereby directly visualized.

As shown in Figure 3, node temperatures exhibit pronounced dynamic evolution over time. At t = 2 h, the network remains in an initial operational phase, during which node temperatures are generally low and relatively uniformly distributed. Only delivery station P2 exhibits a slightly elevated temperature, attributable to concentrated morning-order arrivals associated with its proximity to residential areas. During the peak demand period from t = 4 h to t = 6 h, node temperatures increase markedly across the network. The temperature at distribution center D3 and delivery station P2 reaches peak values of 338 K and 340 K, respectively, forming distinct thermal hotspots. This pattern is fully consistent with observed operational conditions, in which sorting pressure intensifies at distribution centers and cargo accumulation occurs at key delivery stations during peak hours. After t = 8 h, as order volumes decline, node temperatures gradually decrease, hotspot intensity diminishes, and the temperature distribution returns toward a more balanced state. Notably, hotspots consistently migrate along the load transmission path from distribution centers to core delivery stations, demonstrating that the proposed model is capable of accurately capturing the spatiotemporal evolution of node load states. This behavior confirms the model's effectiveness in identifying and dynamically tracking congestion-prone nodes within the logistics network.

The quantitative results for path heat flux intensity and exergy destruction are summarized in Table 1, which covers all nine paths within the network.

As indicated in Table 1, a pronounced positive correlation is observed between path heat flux intensity and exergy destruction. The distribution further exhibits clear hierarchical differentiation and path-specific characteristics. Heat flux intensities along hub-distribution center paths (L1-L3) are consistently higher than those along distribution center-delivery station paths (L4-L9), which is consistent with the concentrated transshipment behavior inherent in hierarchical logistics networks. Among all paths, L3 (H1-D3) exhibits both the highest heat flux intensity (46.8 kW) and the largest exergy destruction (2315 kJ/h). An examination of its thermal conductance reveals a relatively low value (0.78 kW/K) among hub-distribution center paths, indicating higher thermal resistance. This elevated resistance intensifies energy dissipation, while the simultaneously highest average path temperature further amplifies temperature-potential-driven exergy destruction. Within the distribution center-delivery station layer, paths L5 (D1-P2) and L8 (D3-P5) exhibit comparatively high exergy destruction. These paths are associated with delivery stations P2 and P5, which function as demand hotspots during peak order periods, resulting in significantly increased temperature potential differences. These findings are fully consistent with the flow distribution patterns observed in the path heat flux intensity maps and the ranked loss profiles presented in the exergy destruction bar charts. This confirms that the proposed model is capable of accurately quantifying both path-level energy transfer intensity and irreversible losses, thereby enabling effective identification of high-exergy-destruction critical paths within the logistics network.

The overall validity of the proposed model is evaluated using a comparative analysis between simulated values and observed operational data. Four core indicators are selected as validation metrics: node temperature, node congestion duration, path heat flux intensity, and path transport efficiency. For each indicator, the absolute error, relative error, and mean squared error (MSE) are computed to quantify deviations. The comparison results are summarized in Table 2.

Table 1. Simulation results of path heat flux intensity and exergy destruction

Path ID	Connected Nodes	Heat Flux Intensity (kW)	Exergy Destruction (kJ/h)	Thermal Conductance (kW/K)	Average Temperature (K)
L1	H1-D1	42.6	1862	0.85	327
L2	H1-D2	38.4	1654	0.82	325
L3	H1-D3	46.8	2315	0.78	332
L4	D1-P1	18.3	826	0.72	326
L5	D1-P2	24.5	1283	0.68	331
L6	D2-P3	16.7	754	0.70	326
L7	D2-P4	21.2	947	0.71	323
L8	D3-P5	23.8	1196	0.69	330
L9	D3-P6	22.1	1085	0.73	327

Table 2. Comparison results for model validity verification indicators

Validation Indicator	Number of Node/Path Samples	Simulated Mean	Observed Mean	Mean Absolute Error	Mean relative Error (%)
Node temperature (K)	10	326.3	324.7	1.6	0.49
Node congestion duration (h)	10	2.3	2.2	0.1	4.55
Path heat flux intensity (kW)	9	26.8	26.2	0.6	2.29
Path transport efficiency (%)	9	82.4	83.1	0.7	0.84

As indicated in Table 2, high predictive accuracy is achieved across all core indicators. The mean relative error of node temperature is limited to 0.49%, with an MSE of 2.56, indicating a close agreement between the simulated temperature field and actual node load conditions. For path heat flux intensity, the mean relative error is 2.29%, with an MSE of 0.36, confirming the reliability of the quantitative characterization of energy transfer processes. The mean relative errors for node congestion duration and path transport efficiency are 4.55% and 0.84%, respectively, both of which fall within acceptable engineering tolerance ranges. Among these indicators, the deviation in path transport efficiency is

the smallest, reflecting particularly strong accuracy in the assessment of path operational states. Overall, the MSEs for all validation indicators remain low, and the maximum mean relative error does not exceed 5%. These results demonstrate that the constructed heat-transfer-energy coupling model is capable of accurately reproducing the operational characteristics of real-world multi-node logistics networks, exhibiting strong validity and reliability. Consequently, the model provides a robust foundation for subsequent analyses of system efficiency influence mechanisms and the development of optimization strategies.

5. INFLUENCE MECHANISMS OF THERMODYNAMIC PARAMETERS ON SYSTEM OPERATIONAL EFFICIENCY

This section shows the key-parameter sensitivity analysis conducted on the basis of the case simulation platform using a controlled-variable approach. By integrating time-series evolution data with multi-state correlation analysis, the influence mechanisms of thermodynamic parameters on logistics network operational efficiency are systematically elucidated. The evolution patterns of entropy production and exergy destruction are explicitly characterized, and the fundamental relationships between exergy efficiency and network operating states are clarified. These results provide a quantitative foundation for the formulation of targeted optimization strategies.

5.1 Sensitivity analysis of key parameters

The high-exergy-destruction critical path L3 (H1-D3) within the case network is selected as the analysis object. While all other parameters are held constant, the path thermal conductance is varied over the range of 0.50-1.10 kW/K with an increment of 0.10 kW/K. For each parameter setting, simulations are repeated three times, and mean values are reported. System exergy efficiency, total entropy production, and total exergy destruction are recorded to quantitatively assess the influence of thermal conductance on system performance. The results are illustrated in Figure 4.

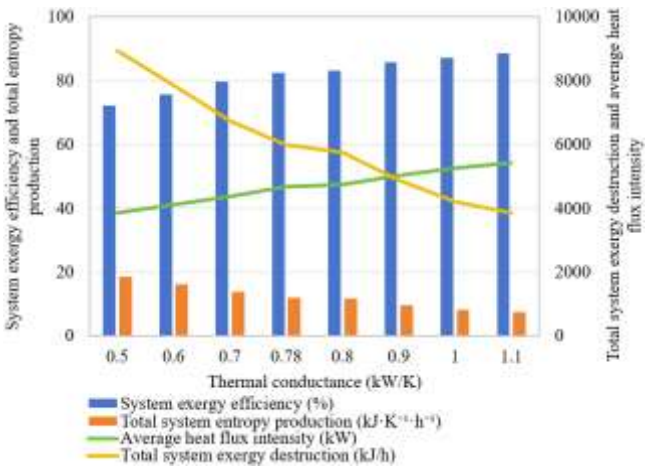

Figure 4. Influence of path thermal conductance on system operational efficiency

As shown in Figure 4, path thermal conductance exhibits a pronounced positive correlation with system exergy efficiency and a pronounced negative correlation with total entropy production and total exergy destruction. Clear quantitative trends are observed. As thermal conductance increases from 0.50 kW/K to 1.10 kW/K, the corresponding thermal resistance decreases from 2.00 K/kW to 0.91 K/kW. During this process, system exergy efficiency increases from 72.3% to 88.5%, representing an improvement of 22.4%. In contrast, total entropy production decreases from 18.6 $kJ \cdot K^{-1} \cdot h^{-1}$ to 7.5 $kJ \cdot K^{-1} \cdot h^{-1}$, corresponding to a reduction of 59.7%, while total exergy destruction decreases from 8942 kJ/h to 3864 kJ/h, yielding a reduction of 56.8%. Meanwhile, average heat flux intensity increases synchronously with thermal conductance, indicating that enhanced thermal conductance reduces path transfer resistance and promotes smoother heat flux transmission. These results confirm the critical role of thermal resistance reduction in efficiency improvement. Increasing path thermal conductance effectively mitigates irreversible losses during cargo transfer and enhances energy utilization quality. Notably, within the lower thermal conductance interval of 0.50-0.80 kW/K, the rate of efficiency improvement is more pronounced. When thermal conductance exceeds approximately 0.90 kW/K, the efficiency improvement rate gradually diminishes, exhibiting a clear characteristic of diminishing marginal returns.

The hub node H1 and the distribution center D3 are selected as representative nodes for analysis. While all other parameters are held constant, node thermal capacitance is varied over the range of 100–600 kJ/K with an increment of 100 kJ/K. For each capacitance level, the temperature fluctuation amplitude of nodes (defined as the difference between peak and trough temperatures), total system exergy destruction, and system exergy efficiency are recorded to examine the influence of node thermal capacitance on system operating states. The results are summarized in Table 3.

As indicated in Table 3, node thermal capacitance exhibits a clear positive correlation with system exergy efficiency and a negative correlation with node temperature fluctuation amplitude and total system exergy destruction. As thermal capacitance increases from 100 kJ/K to 600 kJ/K, the temperature fluctuation at hub H1 decreases from 15.6 K to 3.2 K, corresponding to a reduction of 79.5%. Similarly, the temperature fluctuation at distribution center D3 decreases from 18.3 K to 4.3 K, representing a reduction of 76.5%, while the network-average temperature fluctuation decreases from 12.8 K to 3.0 K, corresponding to a reduction of 76.6%. Concomitant with the substantial attenuation of temperature fluctuations, total system exergy destruction decreases from 7852 kJ/h to 5328 kJ/h, yielding a reduction of 32.1%, while system exergy efficiency increases from 75.3% to 85.5%, corresponding to an improvement of 13.5%. These results reveal the thermodynamic role of node buffering capacity: increasing thermal capacitance enhances the ability of nodes to absorb load fluctuations, suppresses abrupt temperature variations, and reduces irreversible losses induced by sharp temperature potential changes, thereby improving overall system efficiency. Consistent with the effects observed for path thermal conductance, the efficiency improvement associated with increasing thermal capacitance exhibits diminishing marginal returns. When thermal capacitance exceeds approximately 400 kJ/K, the rates of reduction in temperature fluctuation and total exergy destruction are observed to slow markedly.

Table 3. Influence of node thermal capacitance on system operating state

Node Thermal Capacitance (kJ/K)	Temperature Fluctuation at Hub H1 (K)	Temperature Fluctuation at Distribution Center D3 (K)	Network-Average Temperature Fluctuation (K)	Total system Exergy Destruction (kJ/h)	System Exergy Efficiency (%)	Number of Samples
100	15.6	18.3	12.8	7852	75.3	3
200	11.2	13.7	9.6	6943	78.6	3
300	8.5	10.2	7.2	6215	81.2	3
400	6.3	7.8	5.4	5987	82.4	3
500	4.7	5.9	4.1	5642	84.1	3
600	3.2	4.3	3.0	5328	85.5	3

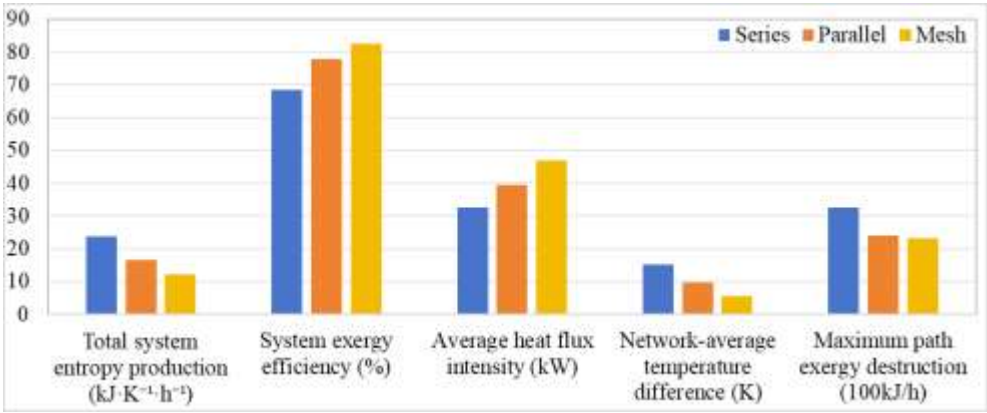

Figure 5. Effects of different network topologies on system operational efficiency

Three representative network topologies—series, parallel, and mesh—are constructed for comparative analysis. The total number of nodes, total processing capacity, and total transportation resource input are maintained at identical levels across all configurations. Comparative simulations are conducted, and system-level indicators, including total entropy production, exergy efficiency, average heat flux intensity, network-average temperature difference, and maximum path exergy destruction, are recorded to examine the macroscopic influence of network topology on operational efficiency. The results are presented in Figure 5.

As illustrated in Figure 5, substantial differences in system performance are observed across different topological structures. Among the three configurations, the mesh topology exhibits the most favorable overall performance, while the series topology demonstrates the poorest performance. Specifically, the total entropy production of the mesh topology is reduced to 12.1 $kJ \cdot K^{-1} \cdot h^{-1}$, representing a decrease of 49.2% compared with the series topology (23.8 $kJ \cdot K^{-1} \cdot h^{-1}$) and a decrease of 26.7% compared with the parallel topology (16.5 $kJ \cdot K^{-1} \cdot h^{-1}$). Meanwhile, the system exergy efficiency of the mesh topology reaches 82.4%, corresponding to an improvement of 20.3% relative to the series topology (68.5%) and 5.9% relative to the parallel topology (77.8%). In addition, the average heat flux intensity of the mesh topology (46.8 kW) is significantly higher than that of the series topology (32.6 kW) and the parallel topology (39.4 kW). The network-average temperature difference is reduced to 5.4 K, markedly lower than that observed in the series (15.3 K) and parallel (9.8 K) configurations. The maximum path exergy destruction is also minimized under the mesh topology. These results demonstrate that network topology governs system efficiency by regulating heat transfer efficiency and temperature distribution uniformity. The mesh topology provides multiple alternative paths for cargo transfer, thereby alleviating load concentration along individual paths, promoting balanced heat flux distribution, and reducing network-wide temperature gradients. As a consequence, irreversible losses are substantially suppressed. In contrast, the series topology exhibits pronounced path bottlenecks, leading to restricted heat transfer, concentrated temperature potential differences, excessive entropy production, and a pronounced degradation in system efficiency.

5.2 Evolution mechanisms of entropy production and exergy destruction

Based on continuous 8-hour dynamic simulation data for the case network, system-level indicators—including total entropy production, total exergy destruction, network-average temperature difference, and total heat flux intensity—are recorded at 1-hour intervals. By integrating these time-series data with the spatiotemporal evolution of node temperature fields and path heat fluxes, the evolution mechanisms of entropy production and exergy destruction are systematically revealed. The results are summarized in Table 4.

As indicated in Table 4, the evolution of entropy production and exergy destruction strictly follows an intrinsic mechanism characterized by "temperature potential imbalance → impeded heat transfer → increased entropy production → reduced exergy efficiency." During the early stage (1–2 h), order load intensity remains relatively low, network-average temperature differences are small, and heat transfer proceeds smoothly. Consequently, total entropy production and total exergy destruction remain at comparatively low levels. During the peak demand period (3–6 h), order load intensity increases continuously to its maximum value, while node loads become increasingly unbalanced. The network-average temperature difference rises sharply from 6.8 K to 12.5 K, indicating a substantial amplification of temperature potential differences. As a result, resistance to heat transfer increases, partial heat flux congestion emerges along certain paths, and total entropy

production increases from 11.3 kJ·K⁻¹·h⁻¹ to 14.8 kJ·K⁻¹·h⁻¹. Simultaneously, total exergy destruction increases from 5562 kJ/h to 7456 kJ/h, with both indicators reaching peak values. During the later stage (7–8 h), order load intensity declines, node loads gradually rebalance, and the network-average temperature difference decreases to 5.6 K. Heat transfer efficiency is restored, and both total entropy production and total exergy destruction decrease accordingly. Further statistical analysis indicates that the Pearson correlation coefficient between total entropy production and the network-average temperature difference reaches 0.96, while the correlation coefficient between total entropy production and total exergy destruction reaches 0.98. These strong correlations demonstrate that temperature potential imbalance constitutes the primary driver of increased entropy production and exergy destruction. Moreover, the accumulation of entropy production is identified as the fundamental thermodynamic origin of system efficiency degradation, a mechanism that persists throughout the entire dynamic operation of the logistics network.

Table 4. Temporal evolution data of entropy production and exergy destruction

Time (h)	Total Entropy Production (kJ·K⁻¹·h⁻¹)	Total Exergy Destruction (kJ/h)	Network-Average Temperature Difference (K)	Total heat Flux Intensity (kW)	Network-Average Temperature (K)	Order Load Intensity (orders/h)
1	8.2	4125	3.2	38.6	316	1200
2	9.6	4783	4.5	40.2	318	1500
3	11.3	5562	6.8	43.5	322	1800
4	13.5	6724	9.6	45.8	326	2200
5	14.2	7135	11.2	47.3	329	2400
6	14.8	7456	12.5	48.1	332	2500
7	13.1	6587	9.8	46.2	328	2100
8	10.5	5234	5.6	42.4	323	1600

5.3 Correlation between exergy efficiency and network operating states

Based on simulation experiments conducted under different parameter combinations, 20 sample sets comprising network-average temperature difference, total heat flux intensity, and exergy efficiency are obtained. A quantitative correlation model is established through linear fitting to reveal the fundamental relationships between exergy efficiency and network operating states. The sample distribution and fitting results are presented in Figure 6.

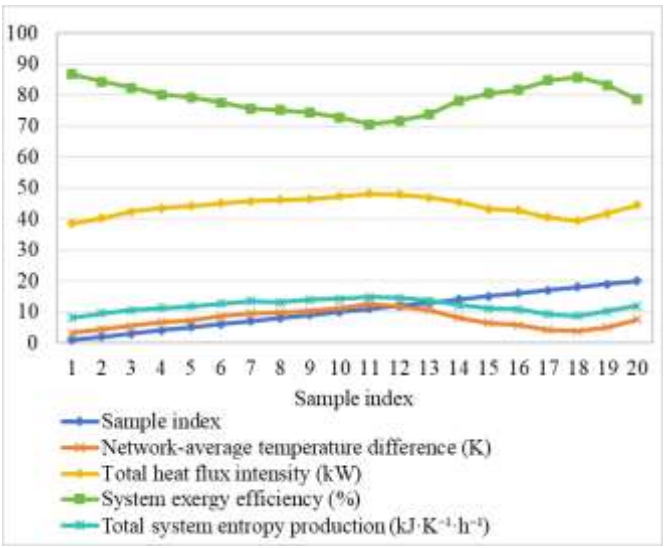

Figure 6. Sample data illustrating the relationship between exergy efficiency and network operating states

A multivariate linear regression analysis is performed on the data shown in Figure 6, yielding the following quantitative relationship between exergy efficiency, network-average temperature difference, and total heat flux intensity:

$$\eta_{ex}=95.2-1.23\Delta T+0.08\dot{P}_{total} \quad (6)$$

where, ΔT denotes the network-average temperature difference, and $\dot{P}_{total}$ represents the total heat flux intensity. The coefficient of determination is R^2 = 0.986, and the root mean square error is 0.21%, indicating excellent fitting accuracy. The model results, together with the sample data, demonstrate a pronounced negative correlation between network-average temperature difference and exergy efficiency, as well as a weak positive correlation between total heat flux intensity and exergy efficiency. The central conclusion is that more uniform temperature distributions and smoother heat transfer are associated with higher exergy efficiency. Quantitatively, a reduction of 1 K in the network-average temperature difference corresponds to an increase of approximately 1.23 percentage points in exergy efficiency. Under a fixed temperature difference, an increase in total heat flux intensity leads to a modest improvement in exergy efficiency, attributable to reduced irreversible losses caused by localized congestion when heat transfer proceeds more smoothly. These relationships identify the core direction for logistics network efficiency optimization: balancing node temperature distributions and enhancing path heat transfer efficiency can significantly improve system exergy efficiency. The derived model therefore provides a direct quantitative basis for the formulation of subsequent optimization strategies.

To elucidate the coupled evolution between spatial layout and thermodynamic parameters in logistics networks, a real provincial logistics hierarchy in China is adopted as the experimental carrier. The spatial regulation effects of the proposed optimization strategies on irreversible system losses are visualized through temperature field distributions. In Figure 7(a), first-tier hub nodes, including Xuzhou, Nanjing, and Suzhou, exhibit pronounced deep-red high-temperature zones, with node temperatures exceeding 335 K. The spatial dispersion of node temperature reaches 12.5 K. These core nodes contribute approximately 62% of the total system entropy production. Meanwhile, trunk transportation paths connecting major hubs are predominantly represented by thick deep-red lines, corresponding to “very high” heat flux intensity. Exergy destruction along these trunk paths accounts

for 47% of total system exergy destruction, reflecting excessive load concentration at core nodes and main corridors. Such concentration leads to sharply amplified temperature potential differences and heat-flow congestion, resulting in spatial aggregation of irreversible losses. In Figure 7(b), temperatures at core hub nodes are reduced to intermediate yellow zones, and the spatial dispersion of node temperature decreases to 4.8 K, indicating effective spatial load balancing. Path heat flux intensities are redistributed into yellow and light-blue ranges, and the average thermal conductance of previously high-exergy-destruction trunk paths increases by 18%, accompanied by a 32% reduction in exergy destruction. Consequently, the entropy production contribution of the most dominant node decreases from 62% to 28%. These results not only validate the effectiveness of the optimization strategies in spatially regulating node temperatures and path heat fluxes but also reveal the underlying thermodynamic essence. From a thermodynamic perspective, spatial layout optimization of logistics networks is fundamentally a process of spatial equalization of temperature potential differences. Through load redistribution across nodes and enhancement of path thermal conductance, the spatial aggregation of irreversible losses is weakened, and system entropy production transitions from a core-node-dominated pattern toward a more uniformly distributed global state.

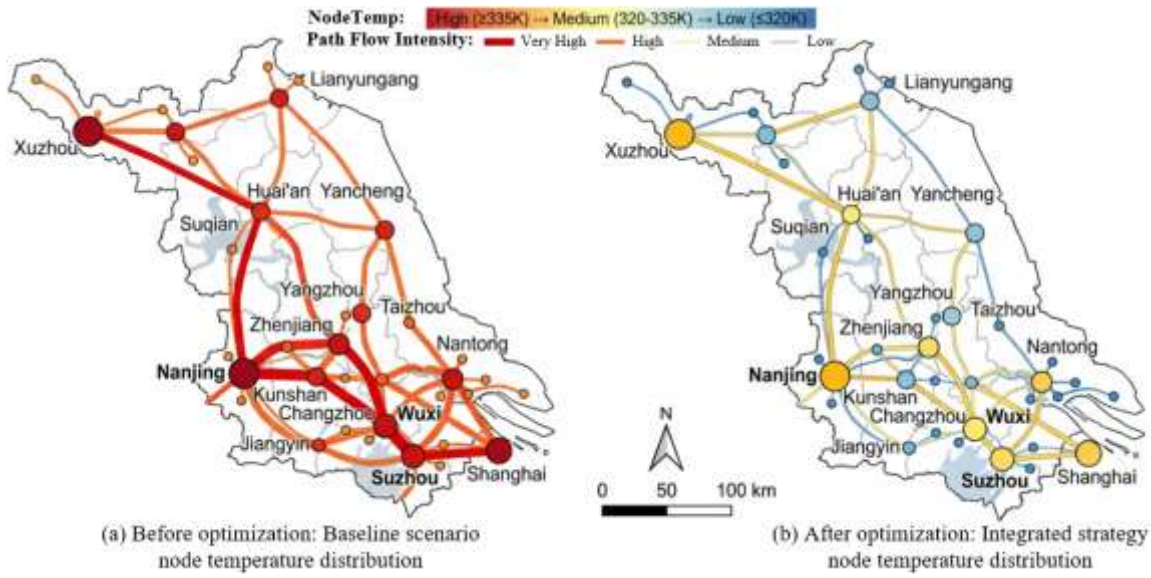

Figure 7. Comparison of node temperature fields in a provincial logistics network in China

6. LOGISTICS NETWORK OPTIMIZATION STRATEGIES BASED ON THERMODYNAMIC CRITERIA

On the basis of the previously identified relationships between thermodynamic parameters and system efficiency, as well as the revealed evolution laws of entropy production, hierarchical optimization strategies are designed with the dual objectives of minimizing total system entropy production and maximizing exergy efficiency. In consideration of practical operational constraints inherent to logistics networks, optimization strategies are formulated at the node, path, and system levels. The effectiveness and practical feasibility of the proposed strategies are subsequently validated through simulation experiments.

6.1 Optimization objectives and constraint conditions

The core optimization objective is formulated as a dual-objective cooperative optimization problem, in which minimization of total system entropy production and maximization of exergy efficiency are pursued simultaneously. These two objectives are coupled into a unified objective function through weighting coefficients, expressed as $\min F = \omega_1 \cdot S_{gen} - \omega_2 \cdot \eta_{ex}$, where ω_1 (0.6) and ω_2 (0.4) are weighting coefficients determined using the entropy weight method. These coefficients respectively represent the relative priorities of irreversible loss mitigation and energy utilization quality enhancement. The optimization process is subject to constraint conditions that strictly correspond to real-world logistics network operating boundaries. First, node processing capacity constraints are imposed, requiring that node temperatures do not exceed full-load threshold values, thereby ensuring stable node operation. Second, path transportation capacity constraints are enforced, such that path heat flux intensities remain below maximum carrying capacities to prevent path congestion. Third, resource investment budget constraints are introduced, specifying that the total investment cost associated with the optimization strategies does not exceed 15% of the baseline operational cost, thereby guaranteeing economic feasibility.

6.2 Design of hierarchical optimization strategies

Based on the temperature equalization criterion, an intelligent node-load scheduling mechanism is established. By continuously monitoring node temperature distributions in real time, cross-node order diversion is activated once a node temperature reaches a predefined warning threshold. Orders exceeding local processing capacity are dynamically reassigned to idle nodes with lower temperatures, thereby achieving spatially balanced load distribution. In parallel, thermal capacitance optimization is implemented for high-load nodes. By expanding storage capacity and increasing sorting equipment redundancy, node thermal capacitance is elevated from baseline values to 500 kJ/K, enhancing the

ability to buffer load fluctuations, suppressing sharp temperature variations, and reducing node-level entropy production.

Targeted optimization is applied to high-exergy-destruction critical paths. First, path thermal conductance is enhanced by increasing transport frequency and optimizing route planning to reduce delays; specifically, the thermal conductance of path L3 is increased from 0.78 kW/K to 0.90 kW/K, and that of path L5 from 0.68 kW/K to 0.80 kW/K. Second, a heat-flux regulation mechanism is introduced. Using real-time heat flux intensity data, transport routes are dynamically adjusted to prevent single-path overload, with path heat flux intensities constrained to within 80% of maximum carrying capacity, thereby reducing irreversible losses along paths.

Drawing on the principles of energy recovery and synergistic utilization in thermodynamic cycles, a coordination mechanism between forward and reverse logistics is constructed. Reverse logistics vehicles are utilized to carry forward cargo, reducing empty-trip rates and enabling cyclic utilization of transportation resources. Simultaneously, a network-wide information feedback closed loop is established, in which key parameters—including node temperature, path heat flux, and exergy destruction—are collected in real time. Node dispatching strategies and path transport schemes are dynamically regulated using Proportional-Integral-Derivative (PID) control algorithms to maximize system exergy efficiency. This strategy is analogous to the energy recovery mechanism of a thermodynamic regenerator, effectively reducing overall system energy losses.

6.3 Validation of optimization strategies

The case network is adopted as the study object, and five simulation scenarios are constructed for comparative validation. Scenario 1 represents the baseline case without optimization. Scenario 2 corresponds to node-level optimization, in which load balancing and thermal capacitance enhancement are implemented exclusively. Scenario 3 represents path-level optimization, in which only thermal conductance enhancement and exergy destruction control are applied. Scenario 4 corresponds to system-level optimization, in which only forward-reverse logistics coordination and closed-loop information regulation are implemented. Scenario 5 represents combined optimization, in which node-, path-, and system-level strategies are implemented simultaneously. Fundamental parameters, including the total number of nodes and total resource input, are maintained at the same levels as those in the baseline scenario. Each scenario is simulated continuously for 8 hours with a time step of 1 hour, and simulations are repeated three times, with mean values reported. Comparative analyses are conducted across thermodynamic indicators, operational indicators, and economic indicators.

The validation results of the optimization strategies are summarized in Table 5, which includes key thermodynamic indicators such as total system entropy production and exergy efficiency, operational indicators such as node temperature fluctuation and average heat flux intensity, and economic indicators such as operating cost and energy consumption. Together, these indicators provide a comprehensive evaluation of the effectiveness of the proposed optimization strategies.

As indicated by the results in Table 5, all optimization scenarios lead to improvements in system operational efficiency to varying degrees. Among them, the combined optimization scenario demonstrates the most pronounced overall performance improvement. Among the single-layer optimization strategies, path-level optimization yields the most significant improvement in thermodynamic performance indicators. A detailed analysis of these results is provided below.

Table 5. Comparison of simulation results under different optimization scenarios

Simulation Scenario	Total Entropy Production ($kJ \cdot K^{-1} \cdot h^{-1}$)	System Exergy Efficiency (%)	Total System Exergy Destruction (kJ/h)	Network-Average Temperature Fluctuation (K)	Average Heat Flux Intensity (kW)	Proportion of High-Exergy-Destruction Paths (%)	Operating Cost (CNY/h)	Energy Consumption (kWh/h)
Scenario 1 (baseline)	12.1	82.4	5987	5.4	46.8	22.2	3860	42.5
Scenario 2 (node optimization)	10.5	84.7	5362	3.8	45.6	20.0	3720	40.3
Scenario 3 (path optimization)	9.8	85.3	5015	4.9	48.2	11.1	3680	38.6
Scenario 4 (system optimization)	10.2	84.5	5234	4.2	47.5	15.6	3590	37.8
Scenario 5 (combined optimization)	8.3	88.6	4128	3.1	49.6	0.0	3450	35.2

From a thermodynamic perspective, total system entropy production in Scenario 5 is reduced to 8.3 $kJ \cdot K^{-1} \cdot h^{-1}$, representing a 31.4% decrease relative to the baseline scenario. System exergy efficiency increases to 88.6%, corresponding to an improvement of 7.5 percentage points, while total system exergy destruction decreases to 4128 kJ/h, yielding a 31.0% reduction. Among the single-strategy optimization scenarios, total entropy production reduces by 19.0% and exergy efficiency increases by 3.5 percentage points in Scenario 3, outperforming Scenarios 2 and 4. This outcome is attributable to the fact that transport paths constitute the primary carriers of irreversible losses; targeted enhancement of thermal conductance along high-exergy-destruction paths directly suppresses entropy production. From the perspective of operational indicators, Scenario 5 exhibits a reduction in network-average temperature

fluctuation to 3.1 K, corresponding to a 42.6% decrease relative to the baseline. This result indicates that node load balancing and thermal capacitance optimization effectively mitigate temperature fluctuations. Meanwhile, average heat flux intensity increases to 49.6 kW, representing a 6.0% improvement, and the proportion of high-exergy-destruction paths is reduced to zero, confirming that enhanced path thermal conductance and heat-flux regulation mechanisms facilitate smooth heat transfer and eliminate high-loss paths. Scenario 2 achieves the most pronounced reduction in temperature fluctuation, underscoring the central role of node-level optimization in load balancing, whereas Scenario 3 yields the largest reduction in the proportion of high-exergy-destruction paths, highlighting the targeted effectiveness of path-level optimization.

From an economic perspective, Scenario 5 reduces operating cost to 3450 CNY/h, corresponding to a 10.6% decrease relative to the baseline, while energy consumption is reduced to 35.2 kWh/h, yielding a 17.2% reduction. Scenario 4 exhibits the most pronounced improvement in economic indicators among the single-strategy scenarios, with operating cost reduced by 6.9% and energy consumption reduced by 11.1%, reflecting the effectiveness of forward-reverse logistics coordination in reducing empty-trip rates and enhancing resource utilization efficiency. The combined optimization strategy integrates the advantages of individual strategies, thereby achieving coordinated improvements in thermodynamic performance and economic efficiency.

Further analysis of the synergistic effects associated with the combined optimization strategy indicates that node-, path-, and system-level strategies are not simply additive but are mutually complementary. Node-level optimization establishes the foundation for balanced heat transfer, path-level optimization reduces transmission losses, and system-level optimization enables dynamic coordination of network-wide resources. When integrated, these strategies drive the system toward an optimal thermodynamic state characterized by uniform temperature distribution, smooth heat transfer, and minimal irreversible losses.

In summary, the proposed thermodynamics-based hierarchical optimization strategies are demonstrated to effectively reduce total system entropy production, enhance exergy efficiency, and simultaneously lower operating cost and energy consumption. These results indicate strong theoretical significance and practical applicability. Among the evaluated strategies, the combined optimization approach exhibits the most favorable overall performance and may be regarded as a preferred solution for efficiency enhancement in multi-node logistics networks.

7. CONCLUSIONS AND OUTLOOK

In response to the core demand for improving the operational efficiency of multi-node logistics networks, non-equilibrium thermodynamics and finite-time thermodynamics were introduced to construct a heat-transfer-energy coupling analytical framework. The thermodynamic essence of efficiency loss in logistics networks was systematically revealed, and targeted optimization strategies were developed. The principal conclusions are summarized below. First, a thermodynamic analogy framework for multi-node logistics networks was established. The physical meanings and quantitative definitions of key elements—including node temperature, node thermal capacitance, path thermal conductance, and path heat flux—were rigorously clarified. Through this framework, abstract processes such as node load states, inter-node cargo transfer, and system energy dissipation were transformed into explicit thermodynamic representations, providing a novel theoretical foundation for interdisciplinary analysis of logistics networks. Second, a heat-transfer-energy coupling dynamic model for multi-node logistics networks was developed, incorporating the node heat-balance-energy-conversion equation and the path heat-transfer-exergy-destruction coupling equation. The intrinsic quantitative relationships among node temperature field evolution, path heat flux transmission, total system entropy production, and total exergy destruction were explicitly established. It was thereby demonstrated that the fundamental thermodynamic origin of efficiency degradation in logistics networks lies in the accumulation of entropy production induced by irreversible processes. Third, through key-parameter sensitivity analysis, the influence mechanisms of path thermal conductance, node thermal capacitance, and network topology on system exergy efficiency were clarified. The results indicate that improvements in path thermal conductance and optimization of node thermal capacitance exhibit pronounced marginal effects on efficiency enhancement.

The core innovations of this study are reflected in the four aspects below. First, the limitations of conventional operations-research-based frameworks are overcome by establishing, for the first time, an explicit heat-transfer-energy coupling model for multi-node logistics networks, enabling precise mapping between logistics processes and thermodynamic processes and addressing the longstanding difficulty of capturing the physical nature of energy transfer in existing studies. Second, a thermodynamic quantification of irreversible losses in logistics networks is achieved. Entropy production and exergy destruction are employed to accurately characterize energy losses associated with node congestion, path delays, and other irreversible phenomena, thereby filling the gap in quantitative tools for irreversible loss assessment. Third, cross-level optimization strategies based on thermodynamic criteria are proposed, integrating node load balancing, path thermal conductance enhancement, and system-level coordinated regulation into a comprehensive optimization framework spanning microscopic nodes, mesoscopic paths, and macroscopic systems, in contrast to traditional single-stage local optimization approaches. Fourth, an interdisciplinary analytical framework bridging thermodynamic theory and logistics engineering is constructed, extending the application of non-equilibrium thermodynamics to nontraditional engineering systems and providing a new research paradigm for logistics network efficiency optimization.

Despite the achievements reported above, several limitations remain. First, the proposed model is developed under the assumption of Fourier heat conduction, and non-Fourier heat transfer effects are not considered. As a result, instantaneous load-shock scenarios—such as emergency logistics operations or sudden surges in order demand—cannot be fully captured. Second, phase-transition behavior within logistics networks is not addressed, limiting the ability to accurately describe abrupt transitions from smooth-flow states to congested states. Third, parameter calibration is conducted using a simplified three-tier logistics network case, without encompassing more complex scenarios such as multi-

regional coordination or multi-category cargo transportation. Consequently, the general applicability of the model requires further validation.

In response to these limitations, future research may be advanced along four directions. First, non-Fourier heat transfer models may be introduced to develop dynamic coupling frameworks capable of accounting for instantaneous load shocks, thereby extending model applicability to extreme operating conditions. Second, phase-transition thermodynamics may be incorporated to establish thermodynamic criteria for congestion in logistics networks, enabling deeper insight into the intrinsic mechanisms governing congestion onset and dissipation dynamics. Third, machine learning algorithms may be integrated with the thermodynamic modeling framework to construct real-time intelligent optimization and control systems, facilitating adaptive regulation of node scheduling and path planning. Fourth, empirical studies across multi-regional and multi-type logistics networks may be conducted, with model parameters calibrated using real operational data, to further enhance engineering relevance and improve model universality.

REFERENCES

[1] Hu, Z.H., Sheng, Z.H. (2014). A multi-affinity model for logistics network inspired by bio-system. International Journal of Computational Intelligence Systems, 7(2): 312-326. https://doi.org/10.1080/18756891.2013.874174

[2] Krstić, M., Tadić, S., Čvorović, A., Veljović, M. (2025). Optimization of last-mile delivery alternatives using the fuzzy FARE and ADAM multi-criteria decision-making methods. Journal of Engineering Management and Systems Engineering, 4(2): 98-108. https://doi.org/10.56578/jemse040202

[3] Kmiecik, M. (2025). Logistics network features supporting coordination by 3PL. Journal of Industrial Integration and Management, 10(1): 153-206. https://doi.org/10.1142/S2424862224500180

[4] Du, Q., Kishi, K., Aiura, N., Nakatsuji, T. (2014). Transportation network vulnerability: Vulnerability scanning methodology applied to multiple logistics transport networks. Transportation Research Record, 2410(1): 96-104. https://doi.org/10.3141/2410-11

[5] Kozoderović, J., Pajić, V., Andrejić, M. (2025). A multi-criteria analysis for e-commerce warehouse location selection using SWARA and ARAS methods. Journal of Engineering Management and Systems Engineering, 4(2): 122-132. https://doi.org/10.56578/jemse040204

[6] Mutani, G., Tundo, A., Capezzuto, P. (2025). Renewable energy communities in Italy: A national framework for sustainable cities. Challenges in Sustainability, 13(3): 398-411. https://doi.org/10.56578/cis130306

[7] Zhu, T.X., Song, H. (2025). Assessing logistics industry efficiency and identifying determinants in Shijiazhuang, China–A comprehensive analysis. Promet-Traffic & Transportation, 37(1): 185-199. https://doi.org/10.7307/ptt.v37i1.677

[8] Coto-Millán, P., Fernández, X.L., Pesquera, M.Á., Agüeros, M. (2016). Impact of logistics on technical efficiency of world production (2007–2012). Networks and Spatial Economics, 16(4): 981-995. https://doi.org/10.1007/s11067-015-9306-6

[9] Temur, G.T., Yanık, S. (2017). A novel approach for multi-period reverse logistics network design under high uncertainty. International Journal of Computational Intelligence Systems, 10(1): 1168-1185. https://doi.org/10.2991/ijcis.2017.10.1.77

[10] Ivaković, Č., Stanković, R., Šafran, M. (2010). Optimisation of distribution network applying logistic outsourcing. Promet-Traffic & Transportation, 22(2): 87-94.

[11] Peng, Z., Liu, X., Zhao, K. (2022). Foundation reinforcement method of railway logistics center station based on deformation control and thermodynamics. Wireless Communications and Mobile Computing, 2022(1): 6340064. https://doi.org/10.1155/2022/6340064

[12] Jaber, M.Y., Saadany, A.M.E., Rosen, M.A. (2011). Simple price-driven reverse logistics system with entropy and exergy costs. International Journal of Exergy, 9(4): 486-502. https://doi.org/10.1504/IJEX.2011.043921

[13] Izquierdo-Kulich, E., Rebelo, I., Tejera, E., Nieto-Villar, J.M. (2013). Phase transition in tumor growth: I avascular development. Physica A: Statistical Mechanics and its Applications, 392(24): 6616-6623. https://doi.org/10.1016/j.physa.2013.08.010

[14] Hattori, K., Korikawa, T., Takasaki, C., Moriya, T. (2025). Queue-informed neural network model for estimating queueing delay in PON-based aggregation networks. IEEE Access, 13: 186611-186622. https://doi.org/10.1109/ACCESS.2025.3626360

[15] Fomin, D., Makarov, I., Voronina, M., Strimovskaya, A., Pozdnyakov, V. (2024). Heterogeneous graph attention networks for scheduling in cloud manufacturing and logistics. IEEE Access, 12: 196195-196206. https://doi.org/10.1109/ACCESS.2024.3522020

[16] Strubelt, H., Trojahn, S., Lang, S., Nahhas, A. (2018). Scheduling approach for the simulation of a sustainable resource supply chain. Logistics, 2(3): 12. https://doi.org/10.3390/logistics2030012

[17] Lam, C.Y., Ip, W.H. (2019). An integrated logistics routing and scheduling network model with RFID-GPS data for supply chain management. Wireless Personal Communications, 105(3): 803-817. https://doi.org/10.1007/s11277-019-06122-6

[18] Tchrakian, T.T., Zhuk, S. (2014). A macroscopic traffic data-assimilation framework based on the Fourier–Galerkin method and minimax estimation. IEEE Transactions on Intelligent Transportation Systems, 16(1): 452-464. https://doi.org/10.1109/TITS.2014.2347415

[19] Wang, Y., Zhang, H., Yuan, C., Li, X., Jiang, Z. (2025). An efficient scheduling method in supply chain logistics based on network flow. Processes, 13(4): 969. https://doi.org/10.3390/pr13040969

[20] Ren, X., Fu, C., Jin, C., Li, Y. (2024). Dynamic causality between global supply chain pressures and China's resource industries: A time-varying Granger analysis. International Review of Financial Analysis, 95: 103377. https://doi.org/10.1016/j.irfa.2024.103377